LAWRENCE
LIVERMORE
NATIONAL
LABORATORY

UCRL-PROC-217798

Modeling and Experimental Investigation of Methylcyclohexane Ignition in a Rapid Compression Machine

William J. Pitz, C. V. Naik, T. Ní Mhaoldúin, Charles K. Westbrook, Henry J. Curran, John P. Orme, J. M. Simmie

December 19, 2005

31st International Symposium on Combustion
Heildelberg, Germany
August 6, 2006 through August 11, 2006

Disclaimer

This document was prepared as an account of work sponsored by an agency of the United States Government. Neither the United States Government nor the University of California nor any of their employees, makes any warranty, express or implied, or assumes any legal liability or responsibility for the accuracy, completeness, or usefulness of any information, apparatus, product, or process disclosed, or represents that its use would not infringe privately owned rights. Reference herein to any specific commercial product, process, or service by trade name, trademark, manufacturer, or otherwise, does not necessarily constitute or imply its endorsement, recommendation, or favoring by the United States Government or the University of California. The views and opinions of authors expressed herein do not necessarily state or reflect those of the United States Government or the University of California, and shall not be used for advertising or product endorsement purposes.

Modeling and Experimental Investigation of Methylcyclohexane Ignition in a Rapid Compression Machine

W. J. Pitz[1], C. V. Naik[2], T. Ní Mhaoldúin[3], C. K. Westbrook[1], H. J. Curran[3], J. P. Orme[3], and J. M. Simmie[3]

[1] Lawrence Livermore National Laboratory, Livermore, CA 94551, USA
[2] The Pennsylvania State University, University Park, PA 16802, USA
[3] National University of Ireland, Galway, Ireland

Corresponding author: William J. Pitz
Lawrence Livermore National Laboratory, L-091
P.O. Box 808
Livermore, CA 94551
Fax: 925-423-8772
Email: pitz1@llnl.gov

Colloquium: Reaction Kinetics

Supplemental data included.

Total Length of paper: 5536
Method of determination: Method 1
Main text: 3682
Equations: 144
References: 664
Figure 1: 144
Figure 2: 92
Figure 3: 130
Figure 4: 75
Figure 5: 164
Figure 6: 167
Table 1: 274
Total: 5536

Modeling and Experimental Investigation of Methylcyclohexane Ignition in a Rapid Compression Machine

W. J. Pitz[1], C. V. Naik[2], T. Ní Mhaoldúin[3], H. J. Curran[3], J. P. Orme[3], J. M. Simmie[3], and C. K. Westbrook[1]

[1] Lawrence Livermore National Laboratory, Livermore, CA 94551
[2] The Pennsylvania State University, University Park, PA 16802
[3] National University of Ireland, Galway, Ireland

Abstract

A new chemical kinetic reaction mechanism has been developed for the oxidation of methylcyclohexane (MCH), combining a new low-temperature mechanism with a recently developed high temperature mechanism. Predictions from this kinetic model are compared with experimentally measured ignition delay times from a rapid compression machine. Computed results were found to be particularly sensitive to isomerization rates of methylcyclohexylperoxy radicals. Three different methods were used to estimate rate constants for these isomerization reactions. Rate constants based on comparable alkylperoxy radical isomerizations corrected for the differences in the structure of MCH and the respective alkane, predicted ignition delay times in very poor agreement with the experimental results. The most significant drawback was the complete absence of a region of negative temperature coefficient (NTC) in the model results using this method, although a prominent NTC region was observed experimentally. Alternative estimates of the isomerization reaction rate constants, based on the results from previous experimental studies of low temperature cyclohexane oxidation, provided much better agreement with the present experiments, including the pronounced NTC behavior. The most important feature of the resulting methylcyclohexylperoxy radical isomerization reaction analysis was found to be the relative rates of isomerizations that proceed through 5-, 6-, 7- and 8-

membered transition state ring structures and their different impacts on the chain-branching behavior of the overall mechanism. Theoretical implications of these results are discussed, with particular attention on how intramolecular H atom transfer reactions are influenced by the differences between linear alkane and cycloalkane structures.

Keywords: methylcyclohexane, rapid compression machine, alkylperoxy isomerization

Introduction

Many chemical kinetic studies in recent years have examined oxidation of n-alkane and branched alkane hydrocarbons [1-4] over the low and intermediate temperature ranges that influence ignition phenomena in many practical combustion systems [5] including spark-ignition, diesel, and homogeneous charge, compression ignition (HCCI) engines. The importance of low temperature oxidation and heat release, and the role of a region of negative temperature coefficient (NTC) are now firmly established. Numerous reaction mechanisms have been developed to describe these processes, which emphasize the central role of alkylperoxy radical isomerization reaction pathways that determine the relative amounts of chain branching, propagation and termination and how these balances change with temperature and pressure.

The reaction sequence, which occurs from about 650K to 850K, in shown in Fig. 1, beginning with abstraction of H atoms from the hydrocarbon RH, producing an alkyl radical R. At these low temperatures, O_2 adds rapidly to R to produce the alkylperoxy radical RO_2, which then abstracts an H atom from within the RO_2 species to produce a hydroperoxyalkyl radical QOOH. This process of alkylperoxy radical isomerization

proceeds via a ring-like intermediate transition state containing 5, 6, 7 or 8 atoms, and the rate of each H atom transfer depends on the number of atoms in this transition state ring and the type of C - H bond that is broken when the H atom is abstracted internally [6].

Each QOOH species produced by RO_2 isomerization subsequently reacts via multiple pathways, including isomerization back to RO_2, cyclization to produce epoxides and OH, C - O bond fission to produce olefins and HO_2, or other essentially chain propagation reactions, or addition of another O_2 to begin the only important series of low temperature reactions that leads to chain branching. For n-alkane and branched alkane fuels, the QOOH products of the 5-membered, 7-membered and 8-membered intermediate ring structures react primarily through chain propagation paths [6, 7], and only the 6-membered ring structure products lead primarily to chain branching via the addition of a second O_2 molecule. Prediction of low and intermediate temperature hydrocarbon ignition therefore requires understanding the relative rates of RO_2 isomerization reactions and particularly the proper balance between propagation and branching pathways.

The principal goal of this work is to study these issues when the fuel is a cycloalkane instead of n-alkane or branched alkane, to see if the analogous reaction pathways have similar influences on the overall chain reaction, and how their rates can be related to those for n-alkanes and branched alkanes. A second motivation is the need for comprehensive reaction mechanisms for cycloalkane fuels to include in surrogates for

practical fuels including gasoline, diesel, and jet fuel in simulations of practical combustors. Since these fuels contain hundreds of hydrocarbon components, it is not possible to represent all of them using detailed reaction mechanisms. Instead, a small number of fuel components can be identified to represent a surrogate for the practical fuel. This surrogate is defined by selecting one or more constituents from each chemical class in the practical fuel. These chemical classes include n-alkanes, iso-alkanes, cyclo-alkanes, alkenes, single ring and polycyclic aromatics, and oxygenates. Cyclo-alkanes are important because they comprise a significant fraction of the hydrocarbons in diesel fuel and jet fuel [8]. With the emergence of oil-sand derived fuels with a larger fraction of cyclo-alkanes than conventional fuels [9], cyclo-alkanes will play a larger future role in practical fuel chemistry.

Limited experimental and chemical kinetic mechanism studies have been made on oxidation of cycloalkanes. Low temperature cyclohexane oxidation was investigated by Walker et al. [10, 11] in a static reactor at 670 to 770K and 15 and 500 torr. They used initial product yields from cyclohexylperoxy radical isomerization to derive RO_2 isomerization rate constants. Lemaire et al. [12] studied low temperature oxidation of cyclohexane in a rapid compression machine, finding that cyclohexane exhibits a two-stage ignition at low temperatures. High temperature oxidation of cyclohexane was investigated by Voisin et al. and Bakali et al. in a stirred reactor at elevated pressures [13, 14]. They developed a detailed mechanism for cyclohexane and validated it at temperatures above 900K and at pressures of 1, 2 and 10 atm. There have been at least two studies of the conjugate olefin of cyclohexane (cyclohexene). Ribaucour et al. [15] experimentally investigated ignition and evolution of cyclohexene in a rapid compression

machine and developed a detailed kinetic model from their measurements. Many of their chemical kinetic pathways are similar to those discussed in this work. High temperature cyclohexene oxidation was studied behind reflected shock waves by Dayma et al. [16], who also developed a detailed chemical kinetic mechanism and validated it, using their experiments.

Low temperature oxidation of methylcyclohexane was investigated for one test condition at an equivalence ratio of 0.4 in a rapid compression machine by Tanaka et al. [17]. They observed two-stage ignition of MCH with an ignition delay time near that of 2-heptene. No developments of detailed chemical kinetic mechanisms for MCH or cyclohexane at low temperature have been carried out previous to the present paper. High temperature MCH oxidation has been studied recently by Orme et al. [18], with a thorough review [19] of previous work including earlier studies of Zeppieri et al. [20] in a flow reactor and McEnally et al. in a laminar diffusion flame [21]. High temperature oxidation of n-propylcyclohexane was studied by Ristori et al. [22] in a stirred reactor at atmospheric pressure. They developed a detailed kinetic mechanism for high temperature oxidation of n-propylcyclohexane and validated it by comparison to their experimental measurements.

Methylcyclohexane is a starting point for development of chemical kinetic mechanisms for other cycloalkanes. To provide a kinetic mechanism valid for the wide temperature ranges required for modeling combustion in engines, we developed a low temperature oxidation mechanism for MCH and merged it with a recent high temperature mechanism [18] to model experiments on MCH ignition in a rapid compression machine.

Experiments

The NUIG rapid compression machine (RCM) has a twin opposed piston configuration described previously [23, 24], resulting in fast compression of little more than 16 ms. Creviced piston heads produce a near-homogeneous post-compression temperature distribution in the combustion chamber [25]. Gases were supplied by BOC Ireland: nitrogen (CP Grade) 99.95%, argon (Research Grade) 99.9995%, oxygen (Medical Grade) 99.5% and were used without further purification. Methylcyclohexane was obtained from Aldrich Chemical Co. Ltd. and was determined to be 99.6% pure using gas chromatographic analysis. To minimize the presence of atmospheric air in the sample, liquid MCH was subjected to several freeze–pump–thaw degassing cycles before being used. Stoichiometric fuel/'air' mixtures were prepared manometrically in a stainless steel container and allowed to homogenize over a 12 hour period. Experiments were carried out at a compression ratio of 10.5:1 with a compression time of approximately 16.6 ms. In order to investigate compressed gas temperatures in the range 680—980 K, two different parameters were adjusted: (i) the diluent gases were varied to alter the overall heat capacity of the fuel and 'air' mixture, resulting in a range of compressed gas temperatures; (ii) a thermostat fitted to the combustion chamber allowed the initial temperature to be varied independently. The compressed gas temperature, Tc, was calculated using experimentally measured compressed gas pressures and the initial temperature and pressure in the chamber. Rather than using the exact geometric compression ratio in the calculation of Tc, the compression ratio was varied slightly such that the calculated compressed-gas pressure matched that measured at the end of compression using the isentropic compression formula. This procedure helped to account for heat losses and blowby in the experiment. The variation of specific heat with

temperature for MCH, O_2 and diluent was included in the calculation. Three diluents were used, 100% N_2, 50% N_2:50% Ar, and 100% Ar, providing enough range in diluent specific heat to cover the targeted range of compressed gas temperature while keeping the compression ratio fixed. Tc was then plotted against the measured ignition delay time, to produce the overall reactivity profiles presented below. Pressure–time data were measured using a pressure transducer (Kistler 603B) and recorded digitally using a personal computer. The ignition delay time was defined as the time from the end of compression to the maximum rate of pressure rise at ignition. In general, we found that the ignition delay times were reproducible to within 5% of one another at each Tc.

Chemical kinetic mechanism

The kinetic mechanism used in this study was developed by adding species and reactions needed for the low and high temperature chemistry of MCH to previously mechanisms for C_1-C_6 [7]. Submechanisms for toluene, benzene and cyclopentadiene were included [26]. High temperature reactions for MCH were added from Orme et al. [18], who had validated that mechanism using measured shock-tube ignition delay times and experimental species histories in a flow reactor [20]. The mechanism development in the present work concerns the low temperature chemistry of methylcyclohexane described below. High temperature and low temperature mechanisms assembled here, together with comparisons with multiple experimental datasets, represent significant progress towards a comprehensive detailed kinetic mechanism for MCH oxidation. The mechanism and thermodynamic data in CHEMKIN format [27] are available as supplemental data.

Thermodynamic properties, reactions paths and reaction rate constants for low temperature oxidation of MCH were estimated. Thermodynamic properties of MCH and species associated with its low temperature oxidation were estimated using THERM [28-30]. Reaction paths and associated reaction rate constants were added to describe low temperature oxidation of MCH as outlined in Fig. 1. These reactions follow the addition of MCH radicals to O_2 and subsequent reactions. Reactions include isomerization to form hydroperoxy-methylcyclohexyl radicals (QOOH), and decomposition of QOOH to cyclic ethers and other products. They also include addition of hydroperoxy-methylcyclohexyl radicals to O_2, isomerization to carbonyl-methylcyclohexyl-hydroperoxides ($HO_2Q'=O$ + OH) and their subsequent decomposition to produce carbonyl-cyclohexoxy radicals and OH radicals.

Selection of reaction rate constants for key reactions

The first reaction step in the low temperature chemistry sequence (Fig. 1) is the addition of molecular oxygen to the MCH radical, which has five isomers denoted in Fig. 2. For radical positions "X" and 1, the rate constant was assumed to be the same as addition of O_2 to a primary and tertiary alkyl radical, respectively [7]. For radical positions 2-4, the rate constant was assumed to be analogous to addition to a secondary alkyl radical [7].

The next low temperature reaction step is the isomerization of methylcyclohexylperoxy radicals. Three different sets of rate constants were tested for these reactions. In the first set, rate constants were estimated based on the reaction rate rules for analogous alkylperoxy isomerizations [7]. When estimating the pre-exponential factors, one must account for changes in the number of internal rotors as RO_2 radicals

move along the reaction coordinate from reactant to transition state. This accounting can be performed using the transition state theory expression from Brocard et al. [31]:

$$A = \frac{e\,k\,T}{h} \text{ x } rpd \text{ x } \exp\left[\frac{3.5\left(\Delta n_{irot}^{\ddagger} + 1\right)}{R}\right] \; s^{-1} \qquad \text{(Eqn. 1)}$$

where A is the pre-exponential factor, e is a mathematical constant, k is Boltsmann's constant, h is Planck's constant, T is temperature, R is the gas constant, rpd is the reaction path degeneracy (number of abstractable H-atoms) and $\Delta n_{irot}^{\ddagger}$ is the change in the number of free rotors as RO_2 radical moves from reactant to transition state. The changes in $\Delta n_{irot}^{\ddagger}$ for methylcyclohexylperoxy and alkylperoxy are illustrated in Fig. 3 for a 5-membered transition state ring isomerization. "R" indicates the location of a free rotor in the radical structure. The cyclohexane ring contains no free rotors because the CH_2 groups are hindered from rotating, due to electrostatic interactions between the H atoms in the ring. It can be seen that in the alkylperoxy radical case, two free rotors are lost as the reactant proceeds to the transition state ($\Delta n_{irot}^{\ddagger} = -2$), while in the methylcyclohexylperoxy case, only one free rotor is lost ($\Delta n_{irot}^{\ddagger} = -1$). Since $\Delta n_{irot}^{\ddagger}$ is one higher for the MCH case, the A-factor must be increased by a factor of 5.8 compared to the n-alkylperoxy case. Extending this analysis to the other ring sizes, $\Delta n_{irot}^{\ddagger}$ is two higher for the six-membered ring and three higher for the seven-membered ring isomerization. This leads to increases in the A-factor of the methylcyclohexylperoxy isomerization by 6, 34, and 200 times (Eqn. 1) compared to the alkylperoxy radical isomerization, when the transition state is on the cyclohexane ring.

The A-factors rules from [7] for 5, 6, and 7-membered ring transition states for alkylperoxy radical isomerization were modified to account for these adjusted number of rotors, giving an A-factor of 5×10^{12} per secondary C-H site for RO_2 isomerizations

occurring on the cyclohexane ring (Table 1). The activation energy was assumed to be unchanged from the alkylperoxy isomerization case to the methylcyclohexylperoxy case. The relative branching fractions of the RO_2 isomerizations at 750K are given in the last column in the Table. The 7-membered rings isomerizations are highly favored with 77% of the isomerization going through this ring size. Ribaucour et al. [15] used a similar rate estimation for RO_2 isomerizations in cyclohexene. Based on their rate constants, 97% of the RO_2 isomerizations go through the 7-membered rings at 750K, consistent with the present formulation. As discussed earlier, 7-membered rings lead to chain propagation paths rather than chain-branching paths associated with 6-membered rings. This dominance of the 7-membered ring isomerizations and the resulting lack of low temperature chain branching produces the poor results described below for this set of reaction rate expressions.

A second set of RO_2 isomerization rates were estimated from the experiments of Gulati and Walker [10]. In their cyclohexane experiments, they determined that the corresponding cyclohexylperoxy isomerization rate constants for 5-, 6-, and 7-membered ring transitions states were 5, 5, and 20 times *slower* at 753 K than their corresponding n-/iso-alkylperoxy isomerizations. This difference was attributed to increased strain in the transition state in the 5- and 6-membered ring compared to the analogous ring in the corresponding n-alkylperoxy transition state. For the six-membered ring, the decrease in isomerization rate for cyclohexylperoxy isomerization was attributed to its occurrence only in the "energetically unfavorable twisted boat form" of the cyclohexylperoxy radical (Fig. 4). The "boat" form allows a more strain free RO_2 isomerization, but it is a less

energetically stable structure by about 5 kcal compared to the "chair" form [10]. Since the differences between alkylperoxy and cyclohexylperoxy rate constants were attributed to enthalpy rather than entropy factors, the activation energies of methylcyclohexylperoxy isomerizations were all increased relative to their alkylperoxy radical counterparts [7] by 2.5, 2.5, and 5.0 kcal/mole for the 5, 6, and 7 membered transition states to account for the reduction of 5, 5, and 20 times observed at 753 K by Gulati and Walker, giving the rate expressions shown in Table 1, while the corresponding A-factors for were kept the same as their n-/iso-alkylperoxy counterparts [7]. For this set of rate constants, the 6-membered ring isomerization is greatly favored (Table 1, last column). Since 6-membered rings lead to chain branching paths, this set of rate constants leads to a pronounced NTC behavior, as discussed below.

A third set of RO_2 isomerization rate constants was based on more recent cyclohexane experiments of Handford-Styring and Walker [11]. They were able to derive both pre-exponential factors and activation energies for cyclohexylperoxy isomerizations by measuring initial product yields at 673, 713, 753 and 773K and comparing cyclohexylperoxy isomerization rates to measured alkylperoxy rates. We used the differences they derived in A-factors and activation energies between alkylperoxy and cyclohexylperoxy isomerization rate constants to modify alkylperoxy isomerization rate constants for methylcyclohexylperoxy. The resultant expressions are shown in Table 1. The rate constants are about twice the Gulati and Walker based rate constants at 750K, and the relative branching fractions are similar to the Gulati and Walker values, with the six-membered ring dominating, and calculations with these rate constants also lead to NTC behavior in MCH reaction.

Results

Ignition delay times measured experimentally in the rapid compression machine are shown as symbols in Figure 5. Three sets of experimental results are included; all three are for stoichiometric MCH/O_2/diluent mixtures, but three different diluents (100% N_2, 50% N_2:50% Ar, and 100% Ar) were used to span the range of temperatures shown, as noted earlier. The small differences in results with when different diluents were used are due to different amounts of heat transfer to the combustion chamber walls as the diluent is varied [32].

Ignition delay times predicted by the kinetic model are shown in Fig. 5 for the three sets of isomerization rate constants. Calculations were carried out at constant volume using SENKIN [27], using experimentally determined compressed gas temperature as initial conditions and neglecting heat losses to the combustion chamber walls. This does not consider any reactions that can occur during the latest portion of the compression stroke, which are quite likely to contribute to the fuel consumption in the cases where the observed ignition delay is very short. The ignition delay times predicted using the "alkylperoxy-based estimates" of RO_2 isomerization rates are much too long at low temperatures and fail to exhibit the negative temperature coefficient behavior observed in the experiments. In contrast, the computed ignition delay times using RO_2 isomerization rate constants from Gulati and Walker [10] and from Hanford-Styring and Walker [11] are in much better agreement with the experimental times. The experimentally observed negative temperature coefficient (NTC) behavior is reproduced

correctly by these models. In Fig. 6, experimental results for stoichiometric mixtures at 10, 15, and 20 atm pressure are shown, together with computed results using the Gulati-Walker-based rate expressions. The trend of decreasing ignition delay times with increasing pressure agrees well between the experiments and the model for the entire temperature range, and a strong NTC behavior is observed at all of the pressures studied.

The ignition delay times predicted by the model are still longer overall than those measured in the experiments by about a factor of two at 750K. We note that neglect of reaction during the compression stroke under the most reactive conditions close to 750K is likely responsible for some of these differences.

Discussion

The present model calculations show that the computed results were most sensitive to the rates of methylcyclohexylperoxy radical isomerization reactions. Three sets of these RO_2 isomerization rate constants for MCH were examined, summarized in Table 1. The first set of rate constants, based on transition state analyses developed to describe similar RO_2 isomerization reactions in n-alkane and iso-alkane molecules, lead to RO_2 isomerizations that mainly proceeded through 7-membered transition state rings. The second and third sets of rate constants, based on the experiments of Walker et al., proceed mainly through 6-membered rings. This result is important because only the 6-membered ring leads to significant chain branching through the sequence,

$$RO_2 \leftrightarrow QOOH \qquad \text{(a)}$$

$$QOOH + O_2 \leftrightarrow O_2QOOH \rightarrow HO_2Q'=O + OH \qquad \text{(b)}$$

$HO_2Q'=O \rightarrow OQ'=O + OH$ (c)

where two reactive OH radicals are generated that accelerate the autoignition process. The 5- and 7-membered ring pathways also include these reactions, but they compete with the chain propagating reaction pathways including

$QOOH \rightarrow Q + HO_2$ (d)

for the 5-membered transition state ring, which is fast because its energy barrier is lower than the highly strained, 5-membered ring isomerization reaction of $O_2QOOH \rightarrow HO_2Q'=O + OH$.

For the 7-membered ring pathway, the chain propagation step,

$QOOH \rightarrow QO + OH,$ (e)

is fast because it goes through a transition state with low ring strain to form a tetrahydrofuran, QO. Thus, the reaction sequence (a, b and c) provides significant chain branching only for the 6-membered ring transition state, and the first set of reaction rates in Table 1 minimizes the role of these reactions and effectively eliminates low temperature chain branching.

The first set of rate constants failed to produce the correct NTC behavior, indicating that using n-/iso-alkane based RO_2 isomerization rate constants, corrected for differences in free rotors, leads to rate constants that produce qualitatively incorrect system behavior for this cycloalkane. There are losses in entropy as the reaction proceeds from reactant to transition state, perhaps due to loss of bending motions of the cyclohexane ring, that are unaccounted for by this approach. The two sets of rates based on experiments with cyclohexane provide enough chain branching through 6-membered transition state rings to reproduce the observed NTC character of the ignition. Electronic

structure and statistical mechanics calculations [33] are needed to better explain the differences in rate constants between n-/iso-alkanes and cyclo-alkanes.

Conclusions

Oxidation of methylcyclohexane has been examined experimentally and computationally in a rapid compression machine. A low-temperature oxidation mechanism for methylcyclohexane has been developed to model the experiments. The computations found that n-/iso-alkane-based estimates of RO_2 isomerization rate constants predicted ignition delay times much too long compared to those measured in the RCM. Rate constants based on experimental results of Walker et al. yielded much better predictions compared to the experiments. These differences were attributed to the greater importance of 7-membered ring isomerizations in the original estimates, compared to 6-membered rings in the Walker-based estimates. Our study indicates that the relative rates of 5-, 6-, and 7-membered ring methylcyclohexylperoxy isomerizations are critical to prediction of ignition delay times in NTC regions.

These reaction pathways continue to be the focus of intense scrutiny and theoretical attention; for example, recent studies have shown [34-36] for ethane and propane that concerted HO_2 elimination reactions of the alkylperoxy radical RO_2, leading directly to Q + HO_2, are much more important than previously believed. Since this path is a propagation step and competes with isomerization and subsequent second O_2 addition reactions, inclusion of concerted elimination reaction steps may have a considerable effect on the overall oxidation mechanism. Studies to date on the RO_2 concerted

elimination reaction have considered only small n-alkane hydrocarbons, so extension to cyclic alkanes is currently uncertain, but the present analysis shows that the important parameter will still be the balance between chain-branching and chain-propagation paths for the different RO_2 radicals produced by the reacting hydrocarbon species.

Acknowledgements

This work was supported by the U.S. Department of Energy, Office of Freedom CAR and Vehicle Technologies and under the auspices of the U.S. Department of Energy by University of California Lawrence Livermore National Laboratory under contract No. W-7405-Eng-48. The authors thank program managers Stephen Goguen and Gurpreet Singh for their support of this work. Ms. T. Ní Mhaoldúin and Prof. John Simmie acknowledge support from the European Union contract NNE5-2001-00869.

References

1. C. K. Westbrook, W. J. Pitz, J. E. Boercker, H. J. Curran, J. F. Griffiths, C. Mohamed and M. Ribaucour, *Proc. Combust. Inst.* 29 (2002) 1311–1318.
2. M. Ribaucour, R. Minetti, L. R. Sochet, H. J. Curran, W. J. Pitz and C. K. Westbrook, *Proc. Combust. Inst.* 28 (2000) 1671-1678.
3. F. Buda, R. Bounaceur, V. Warth, P. A. Glaude, R. Fournet and F. Battin-Leclerc, *Combust. Flame* 142 (1-2) (2005) 170-186.
4. P. Dagaut, *Physical Chemistry Chemical Physics* 4 (11) (2002) 2079-2094.
5. C. K. Westbrook, *Proc. Combust. Inst.* 28 (2000) 1563–1577.
6. H. J. Curran, P. Gaffuri, W. J. Pitz and C. K. Westbrook, *Combust. Flame* 114 (1-2) (1998) 149-177.
7. H. J. Curran, P. Gaffuri, W. J. Pitz and C. K. Westbrook, *Combust. Flame* 129 (2002) 253-280.
8. E. Ranzi, Kinetic Modeling of Real Transportation Fuels, *Fourth Mediterranean Combustion Symposium*, Lisbon, Portugal, 2005.
9. Y. Briker, Z. Ring, A. Iacchelli, N. McLean, P. M. Rahimi and C. Fairbridge, *Energy and Fuels* 15 (2001) 23-37.
10. S. K. Gulati and R. W. Walker, *J. Chem. Soc., Faraday Trans.* 2 (1989) 1799-1812.
11. S. M. Handford-Styring and R. W. Walker, *Phys. Chem. Chem. Phys.* 3 (2001) 2043-2052.
12. O. Lemaire, M. Ribaucour, M. Carlier and R. Minetti, *Combust. Flame* 127 (2001) 1971–1980.
13. D. Voisin, A. Marchal, M. Reuillon, J. C. Boettner and M. Cathonnet, *Combust. Sci. Technol.* 138 (1998) 137-158.
14. A. E. Bakali, M. Braun-Unkhoff, P. Dagaut, P. Frank and M. Cathonnet, *Proc. Combust. Inst.* 28 (2000) 1631–1638.
15. M. Ribaucour, O. Lemaire and R. Minetti, *Proc. Combust. Inst.* 29 (2002) 1303-1310.
16. P. A. G. G. Dayma, R. Fournet, F. Battin-Leclerc,, *Int. J. Chem. Kinet.* 35 (7) (2003) 273-285.
17. S. Tanaka, F. Ayala, J. C. Keck and J. B. Heywood, *Combust. Flame* 132 (1-2) (2003) 219-239.
18. J. Orme, J. M. Simmie and H. J. Curran, *J. Phys. Chem. A* In press (2005).
19. J. M. Simmie, *Progress in Energy and Combustion Science* 29 (6) (2003) 599-634.
20. S. Zeppieri, K. Brezinsky and I. Glassman, *Combust. Flame* 108 266-286.
21. C. S. McEnally and L. D. Pfefferle, *Proc. Combust. Inst.* 30 (2005) 1425-1432.
22. A. Ristori, P. Dagaut, A. E. Bakali and M. Cathonnet, *Combust. Sci. Technol.* 165 (2001) 197-228.
23. W. S. Affleck and A. Thomas, *Proc. Inst. Mech. Eng.* 183 (1969) 365–385.
24. L. Brett, J. MacNamara, P. Musch and J. M. Simmie, *Combust. Flame* 124 (2001) 326–329.
25. J. Würmel and J. M. Simmie, *Combust. Flame* 141 (2005) 417-430.
26. W. J. Pitz, R. Seiser, J. W. Bozzelli, K. Seshadri, C.-J. Chen, I. D. Costa, R. Fournet, F. Billaud, F. Battin-Leclerc and C. K. Westbrook, *Chemical Kinetic Study of Toluene*

Oxidation under Premixed and Nonpremixed Conditions, Lawrence Livermore National Laboratory, UCRL-CONF-201575, (2003).
27. R. J. Kee, Rupley, F.M., Miller, J.A., Coltrin, M.E., Grcar, J.F., Meeks, E., Moffat, H.K., Lutz, A.E., Dixon-Lewis, G., Smooke, M.D., Warnatz, J., Evans, G.H., Larson, R.S., Mitchell, R.E., Petzold, L.R., Reynolds, W.C., Caracotsios, M., Stewart, W.E., Glarborg, P., Wang, C., Adigun, O., Houf, W.G., Chou, C.P., Miller, S.F. *Chemkin Collection*, 3.7.1; Reaction Design, Inc.: San Diego, CA, 2003.
28. E. R. Ritter and J. W. Bozzelli, *Int. J. Chem. Kinet.* 23 (9) (1991) 767-778.
29. T. H. Lay, J. W. Bozzelli, A. M. Dean and E. R. Ritter, *J. Phys. Chem.* 99 (39) (1995) 14514-14527.
30. J. W. Bozzelli, Group additivity data files, private communication, June, 2001.
31. J. C. Brocard, F. Baronnet and H. E. O'Neal, *Combust. Flame* 52 (1983) 25-35.
32. J. Würmel, J. M. Simmie and H. J. Curran, *Int. J. Vehicle Design* (2005) In press.
33. H. Sun and J. W. Bozzelli, *J. Phys. Chem. A* 108 (10) (2004) 1694-1711.
34. C. Y. Sheng, J. W. Bozzelli, A. M. Dean and A. Y. Chang, *J. Phys. Chem. A.* 106 (2002) 7276-7293.
35. H.-H. Carstensen, C. V. Naik and A. M. Dean, *J. Phys. Chem. A.* 109 (2005) 2264-2281.
36. E. G. Estupinan, S. J. Klippenstein and C. A. Taatjes, *J. Phys. Chem. B.* 109 (2005) 8374-8387.

Supplemental data

List of files:

mch_ver1p.mech	text file of MCH mechanism in CHEMKIN format
surrogate_ver8b.therm	text file of MCH thermodynamic properties in CHEMKIN format

Table 1: Methylcyclohexylperoxy radical isomerization rate constants used in present study (cm-mole-sec units; rate constant is per secondary C-H site)

Ring size in transition state	A	n	Ea	Rate at 750K	Branching fraction
Alkylperoxy-corrected estimate:					
5	5.0e12	0	26850	8.0e4	0.4%
6	5.0e12	0	20850	4.5e6	23%
7	5.0e12	0	19050	1.5e7	77%
Gulati and Walker based estimate:					
5	1.00e11	0	29350	3.0e2	12%
6	1.25e10	0	23350	2.1e3	82%
7	1.50e9	0	24050	1.6e2	6%
Hanford-Styring and Walker based estimate:					
5	6.20e10	0	27495	6.0e2	11%
6	1.25e10	0	24076	4.5e3	81%
7	1.50e9	0	24355	4.3e2	8%

List of figure captions:

Fig. 1: Chemical kinetic paths for the low temperature oxidation of alkanes.

Fig. 2: The MCH radical isomers are denoted by a number for a radical site on the ring or "X" for a radical site on the CH_3 group.

Fig. 3: The change in the number of free rotors as an RO_2 radical moves from reactant to a 5-membered transition state for an n-alkylperoxy radical and a methylcyclohexylperoxy radical isomerization.

Fig. 4: The boat and chair structure of the cyclohexylperoxy radical.

Fig. 5: Measured ignition delay times (symbols) for MCH/O_2/diluent stoichiometric mixtures for 10 atm pressure at the end of compression. The predicted ignition delays (curves) are for the three estimates of RO_2 isomerization rates for MCH.

Fig. 6: Comparison of model predictions using the Gulati and Walker based estimate for RO_2 isomerization rates (curves) and experimental measurements (symbols) for stoichiometric mixtures of MCH/O_2/diluent at 10, 15 and 20 atm pressure at the end of compression.

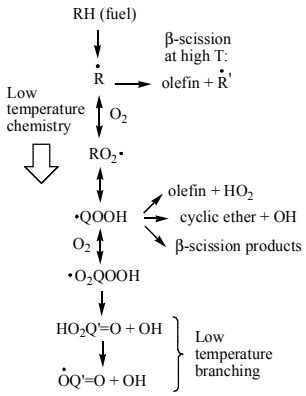

Fig. 1: Chemical kinetic paths for the low temperature oxidation of alkanes.

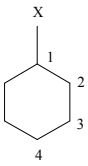

Fig. 2: The MCH radical isomers are denoted by a number for a radical site on the ring or "X" for a radical site on the CH_3 group.

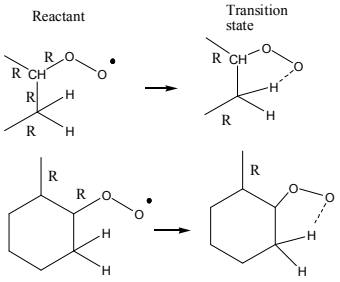

Fig. 3: The change in the number of free rotors as an RO_2 radical moves from reactant to a 5-membered transition state for an n-alkylperoxy radical and a methylcyclohexylperoxy radical isomerization.

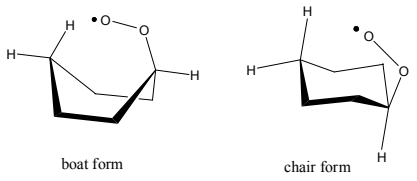

Fig. 4: The boat and chair structure of the cyclohexylperoxy radical.

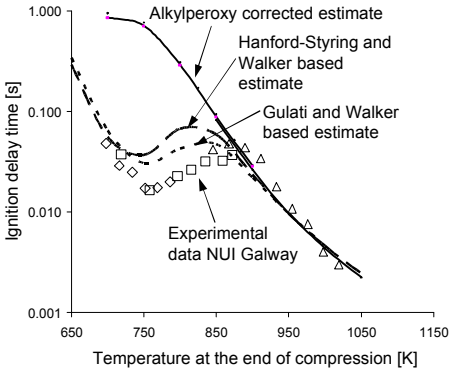

Fig. 5: Measured ignition delay times (symbols) for MCH/O_2/diluent stoichiometric mixtures for 10 atm pressure at the end of compression. The predicted ignition delays (curves) are for the three estimates of RO_2 isomerization rates for MCH.

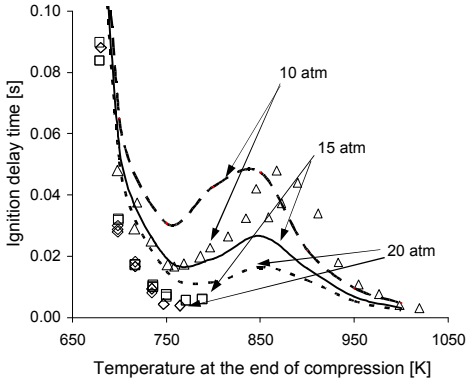

Fig. 6: Comparison of model predictions using the Gulati and Walker based estimate for RO_2 isomerization rates (curves) and experimental measurements (symbols) for stoichiometric mixtures of MCH/O_2/diluent at 10, 15 and 20 atm pressure at the end of compression.